Controlled Coupling of Spin-Resolved Quantum Hall Edge States

Biswajit Karmakar,[1] Davide Venturelli,[1,2,3] Luca Chirolli,[1] Fabio Taddei,[1] Vittorio Giovannetti,[1] Rosario Fazio,[1] Stefano Roddaro,[1] Giorgio Biasiol,[4] Lucia Sorba,[1] Vittorio Pellegrini,[1] and Fabio Beltram[1]

[1]*NEST, Scuola Normale Superiore and Istituto Nanoscienze-CNR, Piazza San Silvestro 12, I-56127 Pisa, Italy*
[2]*Institut NEEL, CNRS and Université Joseph Fourier, Grenoble, France*
[3]*International School for Advanced Studies (SISSA), Via Bonomea 265, I-34136 Trieste, Italy*
[4]*Istituto Officina dei Materiali CNR, Laboratorio TASC, Basovizza (TS), Italy*

(Received 27 July 2011; published 30 November 2011)

We introduce and experimentally demonstrate a new method that allows us to controllably couple copropagating spin-resolved edge states of a two-dimensional electron gas (2DEG) in the integer quantum Hall regime. The scheme exploits a spatially periodic in-plane magnetic field that is created by an array of Cobalt nanomagnets placed at the boundary of the 2DEG. A maximum charge or spin transfer of $28 \pm 1\%$ is achieved at 250 mK.

DOI: 10.1103/PhysRevLett.107.236804 PACS numbers: 73.43.−f, 03.67.−a, 72.10.−d, 72.25.Dc

Topologically protected edge states are dissipationless conducting surface states immune to impurity scattering and geometrical defects that occur in electronic systems characterized by a bulk insulating gap [1]. One example can be found in a clean two-dimensional electron gas (2DEG) under high magnetic field in the quantum Hall (QH) regime [2]. In the integer QH case, spin-resolved edge states (SRESs) at filling fraction $\nu = 2$ (number of filled energy levels in the bulk) are characterized by very large relaxation [3] and coherence [4] lengths. This system is a promising building block for the design of coherent electronics circuitry [4–8]. It represents also an ideal candidate for the implementation of dual-rail quantum-computation architectures [9] by encoding the qubit in the spin degree of freedom that labels two distinct copropagating, energy-degenerate SRESs of the *same* Landau level (LL) at the *same* physical edge of the 2DEG [10]. A key element for the realization of such architecture [10–12] is a coherent beam splitter that makes it possible to prepare any superposition of the two logic states, thus realizing one-qubit gate transformations. This requires the ability to induce controlled charge transfer between the two copropagating SRESs, a goal which up to date has not been yet achieved. Here we solve the problem by targeting a resonant condition, in analogy with the periodic poling technique adopted in optics [13].

In the integer QH regime the SRESs are single-particle eigenstates $\psi_{nks}(x, y) = |s\rangle e^{ikx}\chi_{nk}(y)/\sqrt{L}$ of the Hamiltonian $H = (\mathbf{p} + e\mathbf{A})^2/2m^* + V_c(y) - \frac{1}{2}g^*\mu_B B\sigma_z$ which describes a 2DEG in the (x, y)-plane, subject to a strong magnetic field B in the z direction and confined transversely by the potential $V_c(y)$ [14]. Here, $\mathbf{p} \equiv (p_x, p_y)$ and $\vec{\sigma} \equiv (\sigma_x, \sigma_y, \sigma_z)$ are, respectively, the particle momentum and spin operators, $\mathbf{A}$ is the vector potential, L is the longitudinal length of the Hall bar, while m^* and g^* are the effective electron mass and g factor of the material. Each $\psi_{nks}(x, y)$ represents an electron state of the nth LL with spin projection $s \in \{\uparrow, \downarrow\}$ along the z axis, which is characterized by a transverse spatial distribution $\chi_{nk}(y)$, and which propagates along the sample with longitudinal wave vector k. In our analysis we will focus on a $\nu = 2$ configuration, where the longitudinal electron transport occurs through the SRESs of the lowest LL, i.e., $\Psi_\uparrow \equiv \psi_{0,k_\uparrow,\uparrow}(x, y)$ and $\Psi_\downarrow \equiv \psi_{0,k_\downarrow,\downarrow}(x, y)$ (the values $k_\uparrow$, $k_\downarrow$ being determined by the degeneracy condition at the Fermi energy $E_F = \epsilon_{k_\uparrow} = \epsilon_{k_\downarrow}$ of the corresponding eigenenergies). Specifically in our scheme the two SRESs are separately contacted, grounding $\Psi_\downarrow$ and injecting electrons on $\Psi_\uparrow$ via a small bias voltage V. The spin-resolved currents $I_\uparrow$ and $I_\downarrow$ of the two SRESs are then separately measured at the output of the device, after an artificial charge transfer from $\Psi_\uparrow$ to $\Psi_\downarrow$ is induced during the propagation. Since in general $\Delta k \equiv k_\uparrow - k_\downarrow \neq 0$, $\Psi_\uparrow$ and $\Psi_\downarrow$ support electrons at different wave vectors. Hence any external perturbation capable of inducing charge transfer between them must both flip the spin *and* provide a suitable momentum transfer to match the wave-vector gap Δk. In our scheme we achieve this by introducing a spatially periodic in-plane magnetic fringing field $\vec{B}_\parallel(x, y)$ [15] generated by an array of Cobalt nanomagnet (*magnetic fingers*) placed along the longitudinal direction of the 2DEG; see Fig. 1(a). The system Hamiltonian acquires thus a local perturbation term $\Delta H = -g^*\mu_B\vec{B}_\parallel(x, y) \cdot \vec{\sigma}/2$, which at first-order induces a transferred current $I_\downarrow = (e^2V/h)|t_{\uparrow\downarrow}|^2$, where $t_{\uparrow\downarrow} = (L/i\hbar v)\langle\Psi_\downarrow|\Delta H|\Psi_\uparrow\rangle$ is the associated scattering amplitude, and v is the group velocity of the SRESs. To capture the essence of the phenomenon, consider for instance an array of periodicity λ and longitudinal extension ΔX described by a $\vec{B}_\parallel(x, y)$ field of the form $B_y(y)\cos(2\pi x/\lambda)\hat{y}$ for $x \in [-\Delta X/2, \Delta X/2]$ and zero otherwise (here for simplicity x and z component of $\vec{B}_\parallel$ have been neglected). The corresponding transmission amplitude computed at lowest order in the T-matrix expansion [16] is

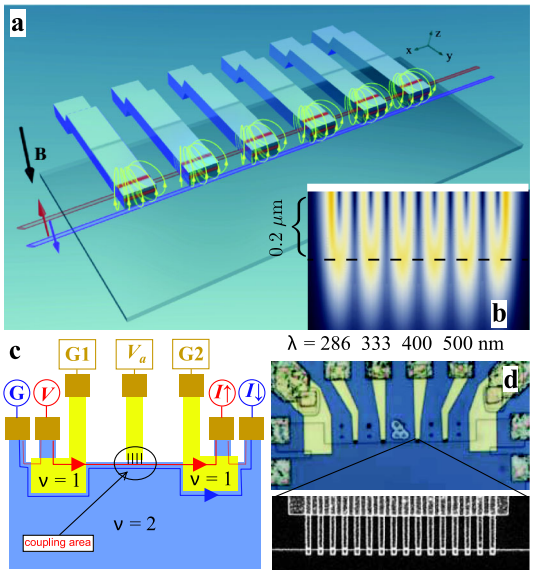

FIG. 1 (color online). (a) Schematics of the device. The Cobalt fingers (blue bars) produce a fringing field (yellow lines) resulting in an in-plane, oscillatory, magnetic field $\vec{B}_{\parallel}$ at the level of the 2DEG (textured gray) residing below the top surface. The field induces charge transfer between the spin up $\Psi_{\uparrow}$ SRES (red line) and spin down $\Psi_{\downarrow}$ SRES (blue line). (b) Density plot of the modulus $\vec{B}_{\parallel}$ in the proximity of the magnetic fingers on 2DEG plane. The dashed line indicates the end of the finger array at 0.2 μm from the physical edge of the mesa (white stripe). (c) Measurement setup: The $\Psi_{\uparrow}$ channel is excited by a bias voltage V, while $\Psi_{\downarrow}$ is grounded at the contact denoted by G. The SRESs can be reversibly decoupled by negatively biasing the array with a voltage V_a ($G1$ and $G2$ are contacts for the top gates). (d) Optical image of the device showing four sets of magnetic fingers with different periodicity λ placed serially at the mesa boundary (the yellow elements are gold eletrical contacts). Zoomed region is the scanning electron microscopic image of the array of periodicity $\lambda = 400$ nm: it is nearly 6 μm long and has an overlap on the mesa of 0.2 μm.

$$t_{\uparrow\downarrow} = ig^{*}\mu_B\langle B_y\rangle\frac{\Delta X}{4\hbar v}\mathrm{sinc}[(2\pi/\lambda - \Delta k)\Delta X/2], \quad (1)$$

with $\mathrm{sinc}[\cdot] \equiv \sin[\cdot]/[\cdot]$ being the sine cardinal function and $\langle B_y\rangle \equiv \int dy B_y(y)\chi_{0,k_{\uparrow}}(y)\chi_{0,k_{\downarrow}}(y)$. The expression clearly shows that even for small values of longitudinal field a pronounced enhancement in interedge transfer occurs when λ matches the wave-vector difference of the two SRESs (i.e., $\lambda_{\mathrm{res}} = 2\pi/\Delta k$), the width of the resonance being inversely proportional to ΔX.

The quantity Δk that defines the resonant condition depends on the Zeeman energy gap and on the details of the confinement potential $V_c(y)$. An estimate based on numerical simulations (see Supplemental Material (SM) [17]) leads to an approximate value $\lambda_{\mathrm{res}} \approx 400$ nm at $B = 4.5$ T, which we assumed as a starting point in designing our setup. The device was fabricated on one-sided modulation-doped AlGaAs/GaAs heterostructure grown by molecular beam epitaxy. The 2DEG resides at the AlGaAs/GaAs heterointerface located 100 nm below the top surface. A spacer layer of 42 nm separates the 2DEG from the Si δ-doping layer above it. The 2DEG has nominal electron density of $2 \times 10^{11}/\mathrm{cm}^2$ and low-temperature mobility nearly 4×10^6 V cm/s. The Cobalt nanomagnet array was defined at the mesa boundary of the 2DEG using e-beam lithography and thermal evaporation of 10 nm Ti followed by 110 nm Co. Eight nanomagnet arrays at different periodicities (specifically $\lambda = 500$, 400, 333, 286, 250, 222, 200, and 182 nm) were fabricated, keeping the total spatial extension of the modulation region nearly constant, $\Delta X \simeq 6.2$ μm [four of them are on the other side of the mesa and therefore not visible in the microscope image of Fig. 1(d)]. The magnetization of the Cobalt fingers is aligned along the applied perpendicular magnetic field B [Fig. 1(a)], if B is large enough [15]. The actual value of the oscillatory $\vec{B}_{\parallel}$ can reach 50 mT in the proximity of the fingers and it decays away from the array [see Fig. 1(b)]. Importantly, coupling between the SRESs and a chosen set of fingers can be activated by increasing the voltage bias V_a of the array from -3 to 0 V [Fig. 1(c)], while keeping all other arrays at $V_a = -3$ V. In these conditions, the SRESs are brought close to the selected array only and exposed to its oscillatory in-plane field $\vec{B}_{\parallel}$. Transport measurements were carried out in a He3 cryosystem with a base temperature of 250 mK equipped with 12 T superconducting magnet. An ac voltage excitation of 25.8 μV at 17 Hz was applied to the electrode V of Fig. 1(c) and the transmitted current was measured by standard lock-in techniques using current to voltage preamplifiers.

We first measured the two-terminal magnetocurrent at $T = 250$ mK in order to locate the plateau associated with a number of filled LLs in the bulk ν equal to 2 [see Fig. 2(a)]. The working point was set in the center of the plateau, i.e., at $B = 4.75$ T. The two SRESs can be separately contacted as schematically shown in Fig. 1(c) by negatively biasing the gates $G1$ and $G2$ at a voltage V_G^*, such that the filling factor below the corresponding top gates becomes $\nu = 1$ and one edge channel only is allowed underneath the gates. The actual V_G^* value can be determined by measuring the currents $I_{\uparrow}$ and $I_{\downarrow}$ as a function of V_G [see Fig. 2(b)]. When interedge coupling is suppressed by applying $V_a = -3$ V to all the nanofingers, we find that spin up electrons are entirely transmitted (yielding a current $I_{\uparrow}$ of about 1 nA, as expected for a single channel of unit quantized resistance $h/e^2 \approx 25.8$ KΩ), while the spin down current $I_{\downarrow}$ is nearly zero for $V_G^* = -0.47 \pm 0.08$ V [see Fig. 2(b)]. In agreement with [3], this implies the absence of significant spin flip processes over the distance of about 100 μm traveled by the copropagating SRESs when the magnetic fingers are deactivated. For completeness, Fig. 2(c) shows the dependence of the currents $I_{\uparrow}$ and $I_{\downarrow}$ on temperature: SRESs fully relax only for $T \sim 1.6$ K (i.e. $1/(k_B\mathrm{T}) \approx 7.2$ meV^{-1}), while edge mixing becomes

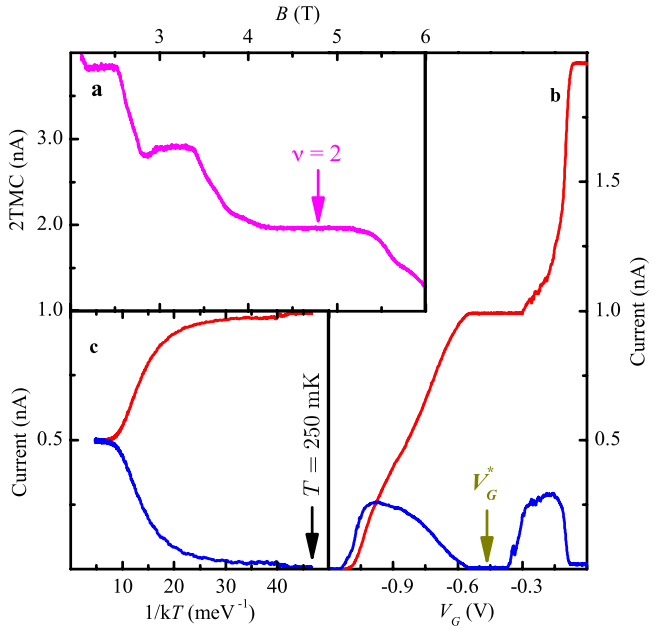

FIG. 2 (color online). (a) Plot of the two-terminal magneto-current (2TMC) measured at 250 mK. The value of magnetic field $B = 4.75$ T, indicated by an arrow, is used to place the 2DEG approximately at the center of the $\nu = 2$ plateau. (b) Plot of the currents $I_\uparrow$ (red) and $I_\downarrow$ (blue) measured at the current terminals red and blue, respectively, [Fig. 1(c)] with the voltage V_G applied to the gates $G1$ and $G2$, while the nanomagnets are deactivated by applying a voltage bias of $V_a = -3$ V to all the arrays. The value of V_G is set to V_G^*, indicated by an arrow, for separately contacting the spin-resolved edge states [see Fig. 1(c)]. (c) Temperature dependence of $I_\uparrow$ (red) and $I_\downarrow$ (blue) currents shows enhancement of relaxation between SRESs with increasing temperature. Thermally mediated mixing of currents becomes negligible at $T = 250$ mK.

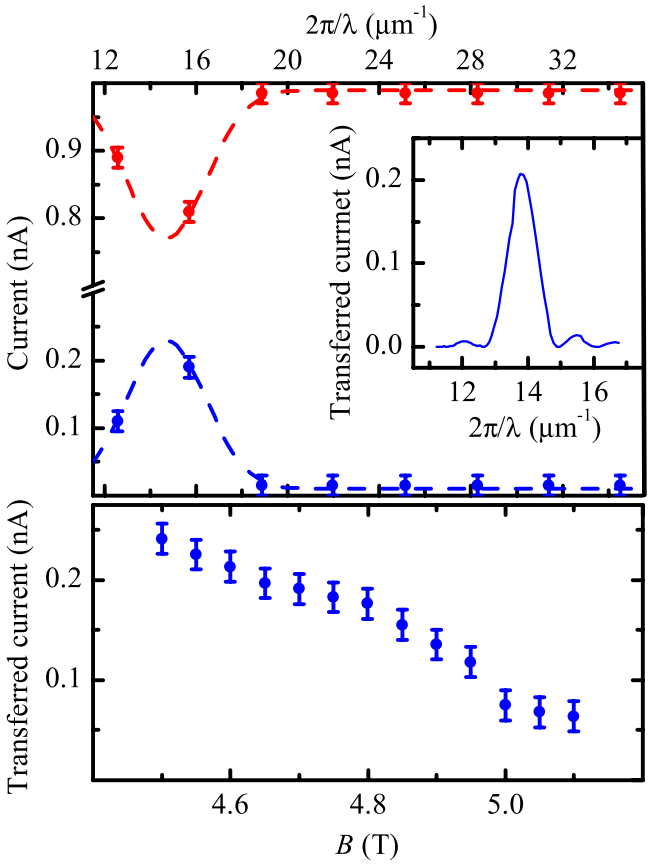

FIG. 3 (color online). Upper panel: Plot of the transmitted currents $I_\uparrow$ (red) and transferred current $I_\downarrow$ (blue) as a function of the inverse periodicity of the activated (by applying $V_a = 0$) set of nanofingers at the working point $B = 4.75$ T and $T = 250$ mK. The measured current $I_\uparrow$ and $I_\downarrow$ are guided by the dashed line which demonstrates selectivity of nanomagnet at periodicity between $\lambda = 400$ nm and 500 nm. The inset shows a numerical simulation of transferred current which in the absence of the static disorder and/or inelastic mechanisms predicts a width of the peak that scales inversely on ΔX as in Eq. (1). Lower Panel: measured transferred current $I_\downarrow$ as a function of the perpendicular magnetic field B for the nanomagnet array of periodicity $\lambda = 400$ nm.

negligible at our working point $T = 250$ mK. Moreover, analyzing our data as in Refs. [3] we can conclude that the relaxation length is of the order of 1 cm at $T = 250$ mK.

The upper panel of Fig. 3 shows the measured $I_\uparrow$ and $I_\downarrow$ when coupling occurs at several different individual arrays (one at a time) as identified by their $2\pi/\lambda$ value. Since interedge coupling leads to charge transfer between the two spin-resolved edge channels it results in a decrease of $I_\uparrow$, with the consequent increase of $I_\downarrow$ while the total current remains constant at about 1 nA. Note that current transfer is significant only for a specific interval of λ values: indeed a resonance peak appears to occur at λ_{res} between 400 and 500 nm. Such behavior is consistent with Eq. (1) and with a more refined theoretical analysis based on the Landauer-Büttiker transport formalism [18] which we have solved numerically in order to go beyond the result of first-order perturbation theory [19] (see inset of the upper panel of Fig. 3 and SM). Static disorder and/or inelastic mechanisms induced, e.g., by the finite temperature and Coulomb interactions, may affect the resonance, resulting in a broadening of the current peak versus $2\pi/\lambda$. Importantly, if the fingers were an incoherent series of scatterers one should expect a monotonic λ dependence of the charge transfer [20], while the observed nonmonotonic selective behavior of the current suggests an underlying constructive interference effect.

For the case of $\lambda = 400$ nm, the lower panel of Fig. 3 shows the dependence of transferred current $I_\downarrow$ on the perpendicular magnetic field B when the latter spans the $\nu = 2$ plateau [see Fig. 2(a)]. The monotonic decrease of $I_\downarrow$ is a consequence of at least three combined effects: (i) the ratio $|\vec{B}_\parallel|/B$ decreases as B is increased, so that the net effect of the in-plane magnetic modulation is weakened; (ii) the magnetic length decreases with increasing B, causing the reduction of the spatial overlap of the transverse

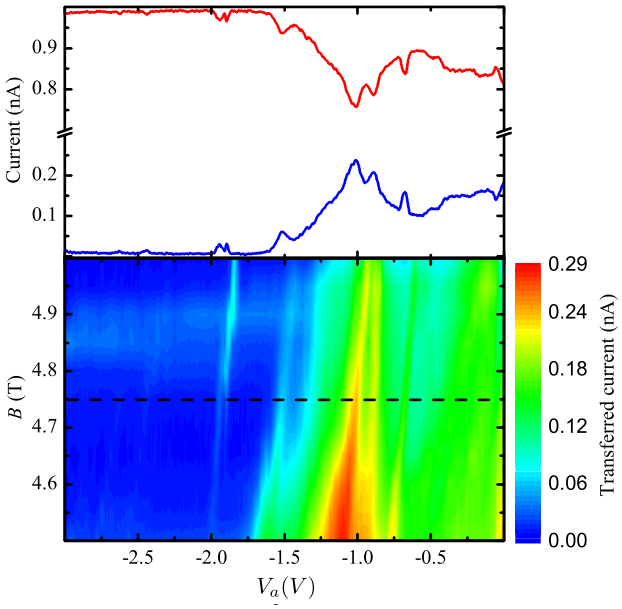

FIG. 4 (color online). Upper panel: Dependence of the transmitted current $I_\uparrow$ (red) and transferred current $I_\downarrow$ (blue) upon the voltage V_a applied to the activated nanofinger set of periodicity $\lambda = 400$ nm at $B = 4.75$ T. For $V_a < -2.0$ V the fingers are effectively decoupled from the SRESs with negligible transfer current; for $V_a \simeq 0$ instead the edges feel the presence of the fingers and a nonzero transfer of current is evident. For intermediate values of V_a a series of pronounced peaks in $I_\downarrow$ are evident. Lower panel: contour plot of $I_\downarrow$ upon V_a and B for the nanofinger set of periodicity $\lambda = 400$ nm. The horizontal dashed line indicates the center of the $\nu = 2$ plateau ($B = 4.75$ T).

wave functions; (iii) the change of SRES spatial configuration with increasing magnetic field due to interaction effects [21,22].

Apart from activating/deactivating the various nanofinger sets, the voltage V_a can also be used as an external control to adjust the resonant mixing condition. Figure 4 shows the measured transferred current $I_\downarrow$ as a function of V_a and B for the array of periodicity $\lambda = 400$ nm (similar data were obtained for different λ, see SM [17]). The pronounced features present for intermediate values of V_a show that the coupling between SRESs can be controlled and amplified. Remarkably, a charge transfer of $28 \pm 1\%$ was achieved at $B = 4.5$ T with $V_a \approx -1.1$ V. At large negative V_a's the SRESs are pushed away from the region where the magnetic fringe field is present and, as expected, the coupling vanishes. The same Fig. 4 reveals additional resonances occurring at specific values of V_a. A nonmonotonic dependence of the local value of Δk on V_a, can be invoked to explain these features. A system simulation shows that a local change of the confinement potential in the proximity of the associated nanofingers modifies the relative distance of the SRESs and hence the local value of Δk in a nonmonotonic way (see SM [17]). More precisely, for low V_a the fingers act as top gates for the underlying edge states: the transverse distance between SRESs can locally increase and reach a maximum as V_a gets negative, since $\Psi_\downarrow$ and $\Psi_\uparrow$ are pushed away from the finger region, one after the other. As we further increase V_a the transverse distance between the SRESs increases again. It is worth stressing, however, that the process just described is not necessarily smooth: electron-electron interaction may in fact induce abrupt transitions in SRESs distances when the slope of the effective local potential decreases below a certain critical value which depends on the details of the sample properties [22] (also the gate voltage can influence the Fermi velocity, as shown in edge magnetoplasmons time-of-flight experiments [23]). The trajectories of SRESs are unknown and [differently from what shown in the graphical rendering of Fig. 1(a)] are likely to be outside the regions corresponding to the projections of the fingers when a significant voltage is applied. Nevertheless nonlinear repulsive effect is expected to be effectively active in the experiment where the electrostatic potential profiles extends much beyond the length of the fingers. Moreover, the functional dependence of the potential induced by V_a upon the longitudinal coordinate x presents also an oscillatory behavior with periodicity λ. As a consequence of the adiabatic evolution of the edges, their transverse distance will also show such oscillations. A detailed modeling of the observed resonance features would require to take fully into account these effects and is beyond the scope of the present Letter. However, it clearly deserves further investigation as it represents a positive feature of the system, since any value of the modulation periodicity λ has typically more than one value of V_a that can fulfill the resonant condition.

Our proposal provides a way to realize beam splitters for flying qubit using topologically protected SRESs. It employs a nanofabricated periodic magnetic field operated at a resonant condition which enhances quite significantly the weak magnetic field produced by the Cobalt nanomagnets. Already at $T = 250$ mK the effect is significant and should be enhanced at lower temperatures.

This work was supported by MIUR through FIRBIDEAS Project No. RBID08B3FM and by EU through Projects SOLID and NANOCTM. We acknowledge useful discussions with N. Paradiso and S. Heun.

[1] C. L. Kane and E. J. Mele, Phys. Rev. Lett. **95**, 226801 (2005); B. A. Bernevig, T. L. Hughes, and S. C. Zhang, Science **314**, 1757 (2006); D. Hsieh *et al.*, Nature (London) **452**, 970 (2008); S. Das Sarma, M. Freedman, and C. Nayak, Phys. Rev. Lett. **94**, 166802 (2005).

[2] K. v. Klitzing, G. Dorda, and M. Pepper, Phys. Rev. Lett. **45**, 494 (1980); D. C. Tsui, H. L. Stormer, and A. C. Gossard, *ibid.* **48**, 1559 (1982).

[3] G. Müller *et al.*, Phys. Rev. B **45**, 3932 (1992); S. Komiyama, H. Hirai, M. Ohsawa, and Y. Matsuda, *ibid.* **45**, 11085 (1992).

[4] Y. Ji *et al.*, Nature (London) **422**, 415 (2003); I. Neder *et al.*, Nature (London) **448**, 333 (2007); Phys. Rev. Lett. **96**, 016804 (2006); **98**, 036803 (2007).
[5] P. Roulleau *et al.*, Phys. Rev. B **76**, 161309(R) (2007); Phys. Rev. Lett. **100**, 126802 (2008); **102**, 236802 (2009).
[6] L. V. Litvin, H.-P. Tranitz, W. Wegscheider, and C. Strunk, Phys. Rev. B **75**, 033315 (2007); **78**, 075303 (2008).
[7] S. Roddaro *et al.*, Phys. Rev. Lett. **103**, 016802 (2009).
[8] E. Bieri *et al.*, Phys. Rev. B **79**, 245324 (2009).
[9] I. L. Chuang and Y. Yamamoto, Phys. Rev. A **52**, 3489 (1995); E. Knill, R. Laflamme, and G. J. Milburn, Nature (London) **409**, 46 (2001).
[10] V. Giovannetti, F. Taddei, D. Frustaglia, and R. Fazio, Phys. Rev. B **77**, 155320 (2008).
[11] T. M. Stace, C. H. W. Barnes, and G. J. Milburn, Phys. Rev. Lett. **93**, 126804 (2004).
[12] C. Nayak *et al.*, Rev. Mod. Phys. **80**, 1083 (2008).
[13] M. M. Fejer, G. A. Magel, D. H. Jundt, and R. L. Byer, IEEE J. Quantum Electron. **28**, 2631 (1992).
[14] R. E. Prange and S. M. Girvin, *The Quantum Hall Effect* (Springer, New York, 1990); D. Yoshioka, *The Quantum Hall Effect* (Springer, New York, 2002).
[15] A. Ursache, J. T. Goldbach, T. P. Russell, and M. T. Tuominen, J. Appl. Phys. **97**, 10J322 (2005); J. U. Bae *et al.*, IEEE Trans. Magn. **44**, 4706 (2008).
[16] M. Di Ventra, *Electrical Transport in Nanoscale Systems* (Cambridge University Press, Cambridge, England, 2008).
[17] See Supplemental Material at http://link.aps.org/supplemental/10.1103/PhysRevLett.107.236804 for a description of the theoretical approach to numerically simulate the transport properties of the proposed device. On this basis we discuss a mechanism that, for a given periodicity of the fingers, produces multiple resonances in the transferred current as we vary the gate voltage V_a. We also report a comparison between the transferred current computed at first order and the exact numerical solution, showing that indeed the former is able to detect the resonant condition and we provide an estimate of the resonant periodicity of the array. Finally, we present some extra data of the measured transferred current as a function of V_a and B for different periodicities λ of the fingers.
[18] M. Büttiker, Phys. Rev. B **46**, 12 485 (1992).
[19] K. Kazymyrenko and X. Waintal, Phys. Rev. B **77**, 115119 (2008).
[20] D. Venturelli *et al.*, Phys. Rev. B **83**, 075315 (2011); N. Paradiso *et al.*, *ibid.* **83**, 155305 (2011).
[21] E. Ahlswede *et al.*, Physica (Amsterdam) **298B**, 562 (2001).
[22] J. Dempsey, B. Y. Gelfand, and B. I. Halperin, Phys. Rev. Lett. **70**, 3639 (1993); L. Rijkels and G. E. W. Bauer, Phys. Rev. B **50**, 8629 (1994).
[23] G. Sukhodub, F. Hohls, and R. J. Haug, Phys. Rev. Lett. **93**, 196801 (2004); H. Kamata, T. Ota, K. Muraki, and T. Fujisawa, Phys. Rev. B **81**, 085329 (2010); N. Kumada, H. Kamata, and T. Fujisawa, Phys. Rev. B **84**, 045314 (2011).